Experimental observation of radial breathing-like mode of graphene nanoribbons

Fang Yu, Haiqing Zhou, Zengxing Zhang, Dongsheng Tang, Minjiang Chen et al.

Citation: Appl. Phys. Lett. **100**, 101904 (2012); doi: 10.1063/1.3692108
View online: http://dx.doi.org/10.1063/1.3692108
View Table of Contents: http://apl.aip.org/resource/1/APPLAB/v100/i10
Published by the American Institute of Physics.

Experimental observation of radial breathing-like mode of graphene nanoribbons

Fang Yu,[1,2,3,a)] Haiqing Zhou,[1,3,a)] Zengxing Zhang,[4] Dongsheng Tang,[5,b)] Minjiang Chen,[1,3] Huaichao Yang,[1,3] Gang Wang,[1,3] Haifang Yang,[6] Changzhi Gu,[6] and Lianfeng Sun[1,c)]
[1]*National Center for Nanoscience and Technology, Beijing 100190, China*
[2]*Academy for Advanced Interdisciplinary Studies, Peking University, Beijing 100871, China*
[3]*Graduate School of Chinese Academy of Sciences, Beijing 100049, China*
[4]*Department of Physics, Tongji University, Shanghai 200092, China*
[5]*College of Physics and Information Science, Hunan Normal University, Changsha 410081, China*
[6]*Institute of Physics, Chinese Academy of Sciences, Beijing 100190, China*

(Received 29 December 2011; accepted 15 February 2012; published online 5 March 2012)

We report that single-walled carbon nanotubes (SWNTs) can be etched into graphene nanoribbons (GNRs) by iron etching, which is confirmed by Raman spectroscopy and transmission electron microscopy. Compared with SWNTs, there are some unique features in Raman spectra of GNRs: symmetric G peak with no splitting, larger Raman intensity of 2D peak than G peak, and lower frequency and narrower full width at half maximum for 2D peak. Similar to radial breathing modes in SWNTs, theoretically predicted radial breathing-like mode of GNRs is also observed: a clear and prominent peak around 223 cm^{-1} in the low frequency regions. This work paves the way for future studies of nanodevices based on SWNT-GNR heterojunction. © *2012 American Institute of Physics*. [http://dx.doi.org/10.1063/1.3692108]

Graphene nanoribbons (GNRs), which are elongated strips of graphene, have attracted theoretical and experimental interests for their potential applications as building blocks in nanodevices and spinelectronics.[1–4] The transformation of carbon nanotubes (CNTs) into GNRs is a very appealing approach because CNTs can be viewed as cylinders of seamless rolling graphene sheets.[5] And the fabrication of GNRs from multi-walled carbon nanotubes (MWNTs) has been reported recently, such as plasma etching,[6] chemical oxidation,[7,8] transition metal nanoparticles cutting,[9] and lithium intercalation and exfoliation.[10] However, it is still a great challenge to cut single-walled carbon nanotubes (SWNTs) into GNRs because of the very small diameter of SWNTs.[11,12]

In this letter, we report on the fabrication of GNRs via iron longitudinal cutting of SWNTs. During thermal annealing, iron particles exhibit directional movements on the SWNTs under the gas coflow of argon (Ar) and hydrogen (H_2). The directional movements of iron particles can result in the cutting of SWNTs into GNRs via catalytic hydrogenation of carbon, which is further confirmed by Raman spectroscopy and transmission electron microscopy (TEM).

Catalytic cutting of MWNTs shows the advantage of much more controllability, such as the metal particle size, kinds of gases, atmospheres, and temperature.[9,13] In order to unzip SWNTs[14] into GNRs, the unique approach used in our experiment is schematically shown in Fig. 1. First, a SWNTs film was put onto a Si substrate with a 300 nm SiO_2 layer, and some wrinkles (thick areas) were found at some regions in the SWNTs film. Second, 5 nm Fe film was thermally deposited onto one end of the SWNTs film in a vacuum thermal evaporator at a deposition rate of 1.0 Å/s under a vacuum of $\sim 10^{-4}$ Pa (Fig. 1(b)). Subsequently, the samples were placed at the center of a quartz tube in a tubular furnace, and a mixed gas of 400 sccm (standard cubic centimeters per minute) Ar and 70 sccm H_2 was introduced. To perform the catalytic hydrogenation of carbon, the center temperature was increased from 25 °C to 900 °C for an hour and kept at 900 °C for about 30 min.[9,15–17]

After thermal annealing, the samples were cooled down to room temperature under the protection of 100 sccm Ar atmosphere. There are several typical features for the morphologies of iron on SWNTs: first, the iron film becomes iron particles with different sizes as shown by region A in Figs. 1(c) and 2(a). Second, iron particles can travel along the SWNTs film where there is no iron film deposited at first (regions B and C). The directional movements of iron particles cannot be observed on the bare substrate where there is no SWNTs film (Fig. 2(b)). Third, there are two kinds of regions on the SWNTs film outside region A: region B with more SWNTs (wrinkles) and C with less SWNTs. In region B, the particle sizes are much larger than those in region C. This indicates that iron particles move faster on region B than C, which is further confirmed by this fact: at the regions far away from iron film, there are iron particles in region B, while no iron particles are found in region C (Fig. 2(c)). These investigations indicate that iron particles have directional movements on the surface of SWNTs.

It is reported that carbon-based materials (graphite, few-layer graphene, and MWNTs) can be etched by thermally activated metallic nanoparticles, such as Fe, Co, and Ni.[9,15,16] Whether can SWNTs be etched into GNRs by the directional movements of iron particles on the surface of SWNTs? Our reply to this question is positive, which is proven from the special Raman spectra of GNRs as well as TEM images.

[a)]F. Yu and H. Zhou contributed equally to this work.
[b)]Electronic mail: dstang@hunnu.edu.cn.
[c)]Electronic mail: slf@nanoctr.cn.

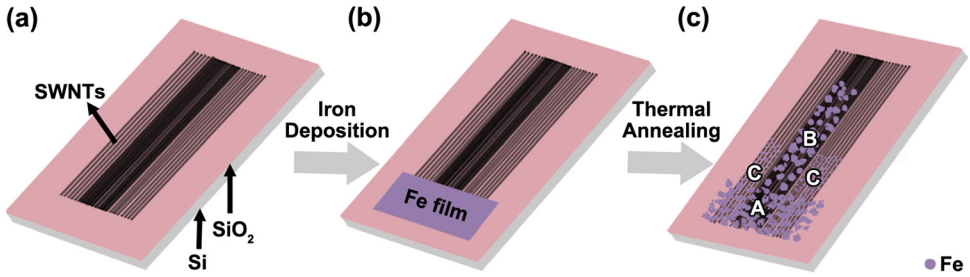

FIG. 1. (Color online) Schematic diagram showing the catalytic hydrogenation process of the SWNTs film by iron etching. (a) Distribution of a SWNTs film onto the SiO_2/Si substrate. Some wrinkles are introduced during this process, which is marked by region B. (b) Thermal evaporation of iron film onto one end of the SWNTs film (region A). (c) Thermal annealing at 900 °C under the mixed gas of Ar and H_2.

Raman spectroscopy is one of the most convenient and credible techniques to investigate the structure and electronic properties of GNRs unzipped from CNTs. The micro-Raman spectroscopy measurements were performed under ambient conditions with 514.5 nm (2.41 eV) excitation from argon ion laser with laser power ~1 mW and laser spot size ~1 μm.

Typical Raman spectra of iron etched SWNTs are shown in Fig. 3, which are found in both regions B and C. For comparison, Raman spectra of annealed SWNTs at the same experimental conditions without iron deposition and as-grown SWNTs are also displayed. The following prominent features can be clearly observed in Raman spectra of iron etched SWNTs: first, the Raman intensity of 2D peak is much stronger than that of G peak, which is obviously different from those of SWNTs. For as-grown or thermally annealed SWNTs without iron, the intensity of G peak is much stronger than 2D peak. The full width at half maximum (FWHM) of 2D peak is about 26.8 cm^{-1} for iron etched SWNTs, which is much smaller than 55.7 cm^{-1} and 47.4 cm^{-1} for as-grown and annealed SWNTs without iron, respectively. This means that the 2D peak shape of iron etched SWNTs is much sharper than that of SWNTs. Second, for iron etched SWNTs, the G peak is symmetric and has no splitting. In contrast, the G peak is composed of two components, such as G^- 1567.3 cm^{-1} (1566.2 cm^{-1}) and G^+ 1591 cm^{-1} (1594.1 cm^{-1}) for as-grown (annealed) SWNTs. Third, the 2D band frequency of iron etched SWNTs is around 2659.2 cm^{-1}, which is consistent with recently reported results for monolayer GNRs from argon plasma etched MWNTs.[6] It is different from 2D peak at 2675.0 cm^{-1} for as-grown SWNTs and 2679.4 cm^{-1} for annealed SWNTs without iron, respectively. These results are similar to those of monolayer graphene,[18,19] indicating that SWNTs can be unzipped into monolayer GNRs by the directional movements of iron particles on the SWNTs. Other features in Raman spectra of iron etched SWNTs, such as the peak (denoted by "▼") at 1513.2 cm^{-1} and the D peak at 1354.1 cm^{-1}, also support the formation of GNRs by iron

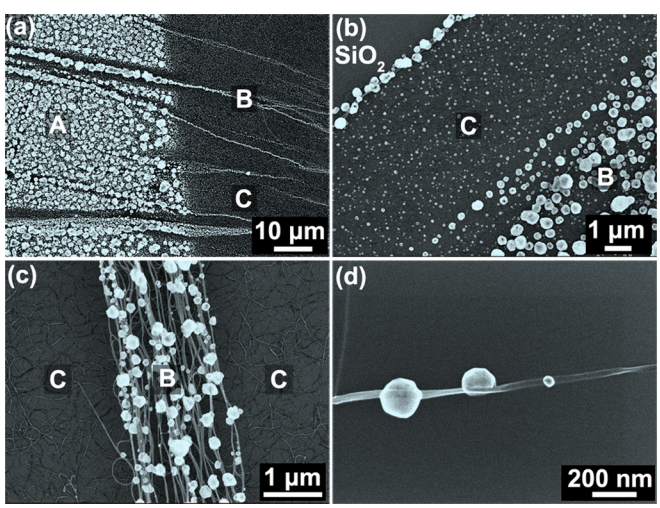

FIG. 2. (Color online) The directional movements of iron particles on the SWNTs and different iron morphologies at different regions of the SWNTs film. (a) Iron source (region A), thick (region B), and thin (region C) SWNTs film. (b) Substrate, thick (region B), and thin (region C) SWNTs film. There are no directional movements of iron particles on the substrate. (c) At the locations far away from region A, there are iron particles at region B and no iron particles at region C. (d) The vivid picture of iron particles traveling on the surface of SWNTs.

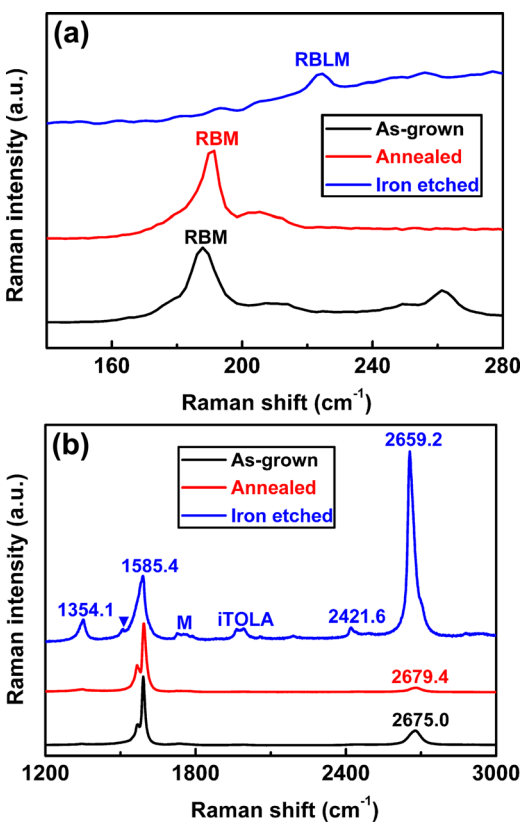

FIG. 3. (Color online) Raman spectra of as-grown SWNTs (bottom), thermally annealed SWNTs without iron deposition (middle) and GNRs (top). (a) Comparison of the RBM in SWNTs with the most characteristic RBLM of GNRs around 223 cm^{-1}. (b) Significant changes in the G and 2D peak shape, frequency, and intensity of GNRs compared with those of SWNTs. These spectra are normalized to the G peak intensity.

cutting. The peak around 1513.2 cm^{-1} can be ascribed to the intrinsic feature of edge atoms of the unzipped GNRs terminated with H atoms.[20] The peak at 1354.1 cm^{-1} is a strong disorder-related band (D), which may be ascribed to the edge effect of GNRs. The peaks denoted by "M" and "iTOLA" are attributed to overtones and combination modes related to graphite, which can be well explained by double-resonance theory.[21]

What is more interesting is the distinct peak around 223 cm^{-1} in the low frequency regions of the Raman spectra of GNRs. This peak is clearly not the radial breathing mode (RBM) of SWNTs as can be seen from Fig. 3(a). We propose that it can be ascribed to the theoretically predicted radial breathing-like mode (RBLM) of GNRs,[22–24] which is a similar mode to the RBM in SWNT. For the RBLM of GNRs, one half atoms of the nanoribbon move in-phase in one direction and the other half in opposite direction. The relative movements between these two half atoms lead to the appearance of a special RBLM, which is Raman active and can be detected experimentally.

The iron etched SWNTs have been further characterized by TEM, which is shown in Fig. 4. Compared with MWNTs,[9] due to the smaller diameters of SWNTs, it is very difficult to determine whether each SWNT has been etched into narrow GNR, since the widths of most GNRs have almost no differences from the diameters of starting SWNTs. In other words, only these GNRs, whose widths are far away from the diameter distribution for as-grown SWNTs, can be determined to be unzipped from SWNTs. As concluded by TEM investigations, it is interesting to note that some iron etched SWNTs show the width around 3.7 nm, which is not in the range of the diameter distribution for as-grown SWNTs as mentioned in our experimental conditions.[13] This width is corresponding to the circumference of the starting SWNTs with a diameter of roughly 1.2 nm, which is close to the dominant diameter 1.3 nm for as-grown SWNTs (see supplementary material[25]). In view of this observation and special Raman features, we think that these carbon-based nanostructures with around 3.7 nm width can be attributed to the resulting GNRs, which are originally unzipped from SWNTs via iron etching. Correspondingly, it is reasonable to obtain the resulting GNRs with narrower widths than 3.7 nm, since the etching process is not so perfect that iron particles just catalytically cut along the axis of SWNTs with no other expense. Also, it is not easy to determine the presence of H atoms at the edges of GNRs. However, according to TEM-based technique, we can also confirm that the SWNTs can be unzipped into GNRs via iron etching.

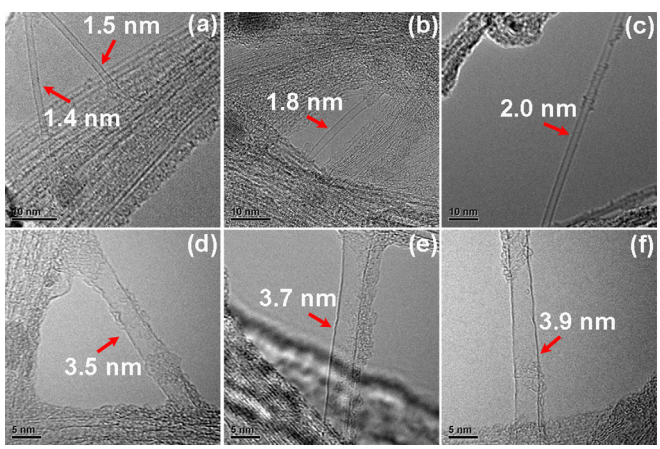

FIG. 4. (Color online) The comparison between the diameter of SWNTs ((a)-(c), scale bar: 10 nm) and the width of GNRs ((d)-(f), scale bar: 5 nm). It is obviously observable that the widths of Fe-etched SWNTs are much larger than the diameters of SWNTs.

To search for the possible mechanism, controlled experiments have been carried out at the same conditions but without H_2 gas. In this situation, iron particles can still move along the SWNTs (Fig. S2(a)[25]). However, the number of SWNTs is almost the same as treated before, and the Raman spectra are similar to that of as-grown SWNTs (Fig. S2(b)[25]). Together with the results of annealed SWNTs, which are treated without iron and other conditions unchanged, this unzipping process can be viewed as a reverse of the SWNTs growth by a chemical vapor deposition method.[9,13] Meanwhile, it is obviously observable that these iron particles distribute well on the surface, rather than locate at one end of our samples (Fig. 2). These indicate that the SWNTs are cut, not dissolved by Fe for the growth of GNRs, and the cutting of SWNTs into GNRs is due to the catalytic hydrogenation of carbon via the movable iron particles on the surface of SWNTs with H_2 presence.

In conclusion, iron particles can move along SWNTs under high temperature. With the presence of H_2 gas, SWNTs can be longitudinally cut into GNRs via catalytic hydrogenation of carbon. The Raman spectra of GNRs show unique modes of RBLM in the low frequency regions and larger intensity of 2D than G peak. The RBLM, which is one of the most characteristic modes in Raman spectra of GNRs, is clearly observed in our experiment. This work has introduced an approach to unzip SWNTs into GNRs and can be useful for fabricating nanodevices based on SWNT-GNR heterojunction.

This work was supported by National Science Foundation of China (Grant Nos. 10774032, 90921001, 11104204 and 50825206), the Program for New Century Excellent Talents in Ministry of Education, China (NCET-07-0278), and Excellent Youth Foundation of Hunan Scientific Committee China (08JJ1001).

[1]W. Y. Kim and K. S. Kim, Nat. Nanotechnol. **3**, 408 (2008).
[2]Z. H. Zhang, C. F. Chen, and W. L. Guo, Phys. Rev. Lett. **103**, 187204 (2009).
[3]F. Muñoz-Rojas, J. Fernández-Rossier, and J. J. Palacios, Phys. Rev. Lett. **102**, 136810 (2009).
[4]K. S. Novoselov, A. K. Geim, S. V. Morozov, D. Jiang, Y. Zhang, S. V. Dubonos, I. V. Grigorieva, and A. A. Firsov, Science **306**, 666 (2004).
[5]L. Tsetseris and S. T. Pantelides, Appl. Phys. Lett. **99**, 143119 (2011).
[6]L. Y. Jiao, L. Zhang, X. R. Wang, G. Diankov, and H. J. Dai, Nature **458**, 877 (2009).
[7]D. V. Kosynkin, A. L. Higginbotham, A. Sinitskii, J. R. Lomeda, A. Dimiev, B. K. Price, and J. M. Tour, Nature **458**, 872 (2009).
[8]Z. X. Zhang, Z. Z. Sun, J. Yao, D. V. Kosynkin, and J. M. Tour, J. Am. Chem. Soc. **131**, 13460 (2009).
[9]A. L. Elías, A. R. Botello-Méndez, D. Meneses-Rodríguez, V. J. González, D. Ramírez-González, L. J. Ci, E. Muñoz-Sandoval, P. M. Ajayan, H. Terrones, and M. Terrones, Nano Lett. **10**, 366 (2010).
[10]A. G. Cano-Márquez, F. J. Rodríguez-Macías, J. Campos-Delgado, C. G. Espinosa-González, F. Tristán-López, D. Ramírez-González, D. A. Cullen, D. J. Smith, M. Terrones, and Y. I. Vega-Cantú, Nano Lett. **9**, 1527 (2009).

[11]L. Y. Jiao, L. Zhang, L. Ding, J. Liu, and H. J. Dai, Nano Res. **3**, 387 (2010).
[12]F. Cataldo, G. Compagnini, G. Patané, O. Ursini, G. Angelini, P. R. Ribic, G. Margaritondo, A. Cricenti, G. Palleschi, and F. Valentini, Carbon **48**, 2596 (2010).
[13]F. Yu, H. Q. Zhou, H. C. Yang, M. J. Chen, G. Wang, and L. F. Sun, Chem. Commun. **48**, 1042 (2012).
[14]Y. C. Zhao, L. Song, K. Deng, Z. Liu, Z. X. Zhang, Y. L. Yang, C. Wang, H. F. Yang, A. Z. Jin, Q. Luo *et al*., Adv. Mater. **20**, 1772 (2008).
[15]L. J. Ci, L. Song, D. Jariwala, A. L. Elías, W. Gao, M. Terrones, and P. M. Ajayan, Adv. Mater. **21**, 4487 (2009).
[16]S. S. Datta, D. R. Strachan, S. M. Khamis, and A. T. C. Johnson, Nano Lett. **8**, 1912 (2008).
[17]L. B. Gao, W. C. Ren, B. L. Liu, Z. S. Wu, C. B. Jiang, and H. M. Cheng, J. Am. Chem. Soc. **131**, 13934 (2009).
[18]H. Q. Zhou, C. Y. Qiu, Z. Liu, H. C. Yang, L. J. Hu, J. Liu, H. F. Yang, C. Z. Gu, and L. F. Sun, J. Am. Chem. Soc. **132**, 944 (2010).
[19]A. C. Ferrari, J. C. Meyer, V. Scardaci, C. Casiraghi, M. Lazzeri, F. Mauri, S. Piscanec, D. Jiang, K. S. Novoselov, S. Roth *et al*., Phys. Rev. Lett. **97**, 187401 (2006).
[20]W. C. Ren, R. Saito, L. B. Gao, F. W. Zheng, Z. S. Wu, B. L. Liu, M. Furukawa, J. P. Zhao, Z. P. Chen, and H. M. Cheng, Phys. Rev. B **81**, 035412 (2010).
[21]V. W. Brar, G. G. Samsonidze, M. S. Dresselhaus, G. Dresselhaus, R. Saito, A. K. Swan, M. S. Ünlü, B. B. Goldberg, A. G. Souza Filho, and A. Jorio, Phys. Rev. B **66**, 155418 (2002).
[22]J. Zhou and J. M. Dong, Appl. Phys. Lett. **91**, 173108 (2007).
[23]R. Saito, M. Furukawa, G. Dresselhaus, and M. S. Dresselhaus, J. Phys.: Condens. Matter **22**, 334203 (2010).
[24]R. Gillen, M. Mohr, and J. Maultzsch, Phys. Rev. B **81**, 205426 (2010).
[25]See supplementary material at http://dx.doi.org/10.1063/1.3692108 for SEM images of as-grown SWNTs, iron particles distributed on SWNTs without H_2 gas, and the corresponding Raman spectra.